



Anti-Proliferative and Pro-Apoptotic Effects of *Calligonum comosum* (L'Her.) Methanolic Extract in Human Triple-Negative MDA-MB-231 Breast Cancer Cells

Zeyad Alehaideb, PhD^{1,2}, Saleh AlGhamdi, PhD^{2,3}, Wesam Bin Yahya, BSc^{1,2}, Hamad Al-Eidi, BSc^{1,2}, Mashaal Alharbi, MSc^{1,2}, Monira Alaujan, MSc^{1,2}, Abeer Albaz, MSc^{1,2} , Muruj Tukruni, BSc^{1,2}, Atef Nehdi, PhD^{2,4}, Maha-Hamadien Abdulla, PhD⁵, and Sabine Matou-Nasri, PhD^{1,2} 

Abstract

Triple-negative breast cancer (TNBC), the most aggressive subtype, does not respond to targeted therapy due to the lack of hormone receptors. There is an urgent need for alternative therapies, including natural product-based anti-cancer drugs, at lower cost. We investigated the impact of a *Calligonum comosum* L'Hér. methanolic extract (CcME) on the TNBC MDA-MB-231 cell line proliferation and related cell death mechanisms performing cell viability and cytotoxicity assays, flow cytometry to detect apoptosis and cell cycle analysis. The apoptosis-related protein array and cellular reactive oxygen species (ROS) assay were also carried out. We showed that the CcME inhibited the TNBC cell viability, in a dose-dependent manner, with low cytotoxic effects. The CcME-treated TNBC cells underwent apoptosis, associated with a concomitant increase of apoptosis-related protein expression, including cytochrome c, cleaved caspase-3, cyclin-dependent kinase inhibitor p21, and the anti-oxidant enzyme catalase, compared with the untreated cells. The CcME also enhanced the mitochondrial transition pore opening activity and induced G₀/G₁ cell growth arrest, which confirmed the cytochrome c release and the increase of the p21 expression detected in the CcME-treated TNBC cells. The CcME-treated TNBC cells resulted in intracellular ROS production, which, when blocked with a ROS scavenger, did not reduce the CcME-induced apoptosis. In conclusion, CcME exerts anti-proliferative effects against TNBC cells through the induction of apoptosis and cell growth arrest. *In vivo* studies are justified to verify the CcME anti-proliferative activities and to investigate any potential anti-metastatic activities of CcME against TNBC development and progression.

Keywords

Calligonum comosum, natural products, triple-negative breast cancer, apoptosis, cell cycle, reactive oxygen species

Received April 14, 2020. Received revised October 29, 2020. Accepted for publication November 10, 2020.

Introduction

Breast cancer has become the most prevalent life-threatening disease in women, estimated as the fifth leading cause of mortality in developed countries, and the second in developing countries due to poor diagnosis.^{1,2} The heterogeneity of this malignancy includes the aggressive triple-negative breast cancer (TNBC) subtype, representing 10%-20% of breast cancers, and characterized by the absence of the expression of hormone receptors and the human epidermal growth factor receptor 2 (HER2).^{3,4} Due to the lack of expression of these receptors, patients with TNBC do not benefit from hormonal therapy (such as estrogen receptor antagonists and aromatase

- ¹ Cell and Gene Therapy Group, Medical Genomics Research Department, King Abdullah International Medical Research Center, Riyadh, Saudi Arabia
- ² King Saud bin Abdulaziz University for Health Sciences, Riyadh, Saudi Arabia
- ³ Clinical Research Department, Research Center, King Fahad Medical City, Riyadh, Saudi Arabia
- ⁴ Department of Medical Research Core Facility and Platforms, King Abdullah International Medical Research Center, Riyadh, Saudi Arabia
- ⁵ Department of Surgery, King Khalid University Hospital and College of Medicine, King Saud University, Riyadh, Saudi Arabia

Corresponding Author:

Sabine Matou-Nasri, Cell and Gene Therapy Group, Medical Genomics Research Department, King Abdullah International Medical Research Center, Riyadh, Saudi Arabia.
 Email: matouepnasrisa@ngha.med.sa



inhibitors) or immuno-therapy targeting HER2 receptors.⁵ The inefficiency of surgery and the severe side effects of conventional anti-cancer therapies pave the way for the development of natural anti-cancer drugs.⁶⁻⁸ Anti-cancer agents derived from plants have prophylactic and therapeutic properties.^{9,10} Due to the toxicity and side effects of current therapeutics, with the high risk of triggering uncontrolled inflammatory reactions due to the dead cancer cells, several natural products are used as complementary and alternative medicine.^{6,11}

The main anti-cancer therapeutic strategies include the induction of natural programmed cell death (apoptosis) and cell growth arrest to reduce the side effects caused by the dead cancer cells.^{6,12-15} Apoptosis can be triggered by the death receptor ligation, with specific ligands or mitochondrial-initiated events activating the extrinsic and intrinsic apoptotic pathways.¹⁶ The extrinsic apoptotic pathway is composed of energy-based enzymatic reactions, resulting in the proteolysis of pro-caspases (inactive forms) into cleaved-caspase (active forms). The intrinsic apoptosis pathway mainly involves mitochondrial-related proteins, such as Bad, and trigger the mitochondrial outer membrane permeabilization for the release of pro-apoptotic components, such as cytochrome c. Both apoptotic pathways converge to the generation of cleaved-caspase-3, the last enzyme that causes membrane reversion (phosphatidylserine exposure), cytoskeletal nuclear protein degradation, and DNA fragmentation.¹⁶ The cell cycle is a strictly regulated process that coordinates cell growth, DNA replication and cell division via checkpoint proteins including cyclin, cell cycle-dependent kinase (cdk) and cdk inhibitors, such as p21.¹⁷ The reactive oxygen species (ROS), short-lived and highly reactive molecules including hydrogen peroxide (H₂O₂), are byproducts of normal cell metabolism and cellular oxidative processes.^{18,19} A high level of ROS generation induce cell death signaling pathways resulting in apoptosis, cell growth arrest and cell death due to damage to the plasma membranes, lipids, proteins, and nucleic acids.²⁰⁻²³

Calligonum polygonoides L. subsp. *comosum* (L'Her.) is a small leafless shrub, which grows in sandy deserts in North Africa and Asia, including Saudi Arabia.²⁴ This plant is traditionally known in the Arabian Peninsula populations as "Ar'ta" (in Arabic, الأرتة) and is primarily used as a natural remedy for stomach ailments and toothache.²⁵ Various *in vivo* experimental studies reported numerous therapeutic properties of *C. comosum*, including anti-ulcerogenic, anti-inflammatory, anti-oxidative stress, and hypoglycemic effects.²⁶ *C. comosum* is rich in flavonoids including (+)-catechin, quercetin, and kaempferol.²⁷ Of note, extracting *C. comosum* compounds with different solvents exert various anti-cancer activities on hepatocarcinoma and the hormone-dependent breast cancer cell line MCF-7.^{28,29} However, there is a knowledge deficit related to the anti-cancer activity of extracted *C. comosum* compounds on non-hormone-dependent TNBC.

We investigated the cytotoxic and anti-proliferative effects of *Calligonum comosum* methanolic extract (CcME) on the non-hormone-dependent TNBC cell line MDA-MB-231. We also investigated the underlying mechanisms of cancer cell

death and the apoptotic pathways occurring in the TNBC cells exposed to CcME.

Materials and Methods

Chemicals and Materials

Quantitative ashless paper filter was provided by Sartorius Stedim Biotech (Göttingen, Germany). Dulbecco's modified eagle medium (DMEM), phosphate buffered saline (PBS), and endotoxin-free water (RNase- and DNase-free) were purchased from UFC Biotechnology (Amherst, NY, USA). Purified carbon dioxide (CO₂) gas was provided by Saudi Industrial Gas (Dammam, Saudi Arabia). Heat-inactivated fetal bovine serum (FBS) was obtained from Gibco® (Thermo Fisher Scientific, Waltham, MA, USA). Triple-negative breast cancer (TNBC) MDA-MB-231 cells were purchased from the American Type Culture Collection (Rockville, MD, USA). Ultra-pure water was produced using a Millipore system (Billerica, MA, USA) with a minimum resistivity of 18.2 MΩ-cm at 25.0°C. All other chemicals were purchased from Sigma-Aldrich (St. Louis, MO, USA), unless otherwise stated.

Source of *Calligonum Comosum*

The aerial part of *C. comosum* was obtained from a local vendor in Riyadh, the central region of Saudi Arabia. The sample was authenticated by Prof. Mona Al-Wahaibi from the Department of Botany and Microbiology, Faculty of Science, King Saud University (KSU), Riyadh, Saudi Arabia. A voucher specimen was deposited at the KSU herbarium, with registration number 24328, for future reference.

Extraction Method of *Calligonum Comosum*

The herbal sample was extracted using high-purity methanol through sonication. Briefly, the sample was grounded to a fine powder using a typical household electrical herb grinder. Approximately 0.1 g of the powder sample was mixed with 10 mL of methanol using the Vibra-Cell™ Ultrasonic Liquid Processor (Model GEX-130, Sonics, Newtown, CT, USA) for 30 min at maximum power. The sonicated extract was filtered using a quantitative ashless paper filter. The filtered extracts were left to evaporate overnight in an oven at 40°C. After determining its extract yield percentage (13.4 ± 3.9%), the methanolic extract was dissolved in 0.5 mL dimethyl sulfoxide (DMSO) by vortex until completely dissolved. After removing bacterial endotoxins from the CcME solution using Pierce™ high capacity endotoxin removal spin columns (Thermo Scientific, Rockford, MA, USA), the level of endotoxins in CcME solution was evaluated using the Pierce™ LAL chromogenic endotoxin quantitation kit (Thermo Scientific), according to the manufacturer's instructions, which were below contamination levels (<0.125 EU/mL). The endotoxin-free CcME solution was kept in the dark at 4°C until use.

Chromatography Fingerprinting

The extracted herbal specimen was analyzed chromatographically using (+)-catechin, quercetin, and kaempferol as the quality phytochemical markers for *C. comosum*. The high-performance liquid chromatography (HPLC) system consisted of a 1290 Infinity II LC System (Agilent Technologies, Santa Clara, CA, USA), equipped with an ultra-violet detector and controlled by Agilent ChemStation data software. The gradient method was based on a published method with

slight modifications.²⁶ Briefly, the fingerprinting was performed using a linear gradient of methanol and ultra-pure water. The gradient started with 5% methanol for 3 min to 100% methanol in 30 min. A wash-period of 100% methanol was maintained for 5 min, followed by an equilibrium period for 5 min with 5% methanol. The injection volume was 10 μ L at ambient temperature and the wavelength was set at 325 nm without reference. The total analysis time was 38 min, including the washing period.

TNBC Cell Culture and Treatment

The TNBC MDA-MB-231 breast cancer cell line was cultured in complete medium, as described in.³⁰ The TNBC cells ($0.25 \times 10^6/\text{cm}^2$, unless otherwise mentioned) were seeded in tissue culture plates (Corning Inc., Corning, NY, USA). The next day, the cells were exposed or not exposed to 1.8% DMSO (concentration detected in 200 μ g/ml CcME and reported to be non-toxic,³¹) or different concentrations (25-200 μ g/mL) of CcME for 24 h incubation.

TNBC Cell Viability Assay

The TNBC MDA-MB-231 cells ($1.5 \times 10^4/\text{cm}^2$) were seeded in a 96-well Greiner® plate and the cell treatment done as mentioned. The wells containing the cells with only complete medium were the controls. The cell viability was measured with a CellTiter-Glo® luminescent cell viability assay kit (Promega Corporation, Madison, WI, USA) as described in.³²

TNBC Cytotoxicity Assay

The TNBC MDA-MB-231 cells ($1.5 \times 10^4/\text{cm}^2$) were plated and treated in complete medium and incubated for 24 h, as described. Cytotoxicity was measured with a Promega CytoTox-Glo® assay kit, following the manufacturer's recommendations. Briefly, the cytotoxicity evaluation was based on the measurement of the fluorogenic cell-impermeant peptide substrate, generated by the released dead-cell protease due to membrane integrity loss. The fluorescent signal was measured using an EnVision™ microplate reader.

Fluorescence-Activated Cell Sorter (FACS) Analysis

The status of apoptosis of the untreated and treated TNBC MDA-MB-231 cells was defined using a Becton Dickinson (BD) Annexin V apoptosis detection kit (BD Biosciences, San Jose, CA, USA) as described in,³² based on the double staining fluorescein isothiocyanate (FITC)-labeled phosphatidylserine-binding protein Annexin V and phycoerythrin (PE)-labeled propidium iodide (PI), an intercalating DNA dye.

The TNBC cell cycle distribution was analyzed based on the DNA amount, stained by PI as described in.³³

The impact of the ROS generated in the CcME-induced apoptosis, was investigated after pre-treating the TNBC cells with 5 mM of antioxidant agent N-acetylcystein (NAC) for 1 h incubation. This was followed by a treatment with either 200 μ g/mL of CcME or 100 nM of protein kinase inhibitor staurosporine, used as a positive control for the induction of apoptosis. After 24 h incubation, the cells were stained to determine the status of apoptosis, as previously described.

Confocal Laser Scanning Microscopy

The TNBC MDA-MB-231 cells were seeded in a Nunc™ Lab-Tek™ 8-well slide chamber system (Thermo Fisher Scientific, Waltham, MA, USA), and treated with CcME as described above. The activity of the mitochondrial permeability transition pore, which allows cytochrome c release, was determined using the Image-iT® LIVE Mitochondrial Transition Pore Assay kit, according to the manufacturer's instructions (Molecular Probes Inc., Life technologies, Carlsbad, CA, USA). The increased permeability of the outer mitochondrial membrane was visualized with a Leica TCS SP8 fluorescence microscope system (Leica Biosystems, Wetzlar, Germany).

Western Blot Analysis

After the protein extraction from the untreated and treated TNBC MDA-MB-231 cells, 35 pro-apoptotic and anti-apoptotic proteins were detected, using the Proteome Profiler Human Apoptosis Protein Array kit (Life Technologies) and analyzed, as described in.³⁴

From cell lysis to the separation, by molecular weight, of the extracted proteins on 12% SDS-PAGE gel electrophoresis, Western blot technology was done as described in.³⁵ Provided by Abcam (Cambridge, UK), mouse monoclonal antibody against pro- and active cleaved-caspase-3 [ABM1C12], rabbit monoclonal antibody against p21 [EPR3993] (1:1000) and mouse monoclonal antibody against GAPDH (1:2000), were used as the primary antibodies for the detection of the targeted proteins. The expression of the targeted proteins was visualized and analyzed as described in.³⁵

TNBC Cellular Reactive Oxygen Species (ROS) Generation Assay

Untreated and treated TNBC MDA-MB-231 cells ($1.5 \times 10^4/\text{cm}^2$) were seeded in a 96-well plate, appropriate for a red fluorescence examination in live cells. The following day, the cells were exposed for 90 min to H₂O₂ (strong inducer of ROS generation), DMSO, or various doses (25-200 μ g/mL) of CcME. To assess the intracellular ROS generation, a cellular ROS detection assay kit (Abcam) was performed as instructed by the manufacturer.

Statistical Analysis

The data are expressed as the mean \pm standard deviation (SD), based on 3 separate experiments. To compare 2 groups, an unpaired Students *t*-test was used. The value of $p < 0.05$ was considered as statistically significant.

Results

Concentrations of the Selected Flavonoids in CcME

The fingerprinting of CcME was performed to authenticate the sample and quantify the selected flavonoids in the extract for comparison and quality control purposes. The chemical analysis of the CcME, based on the content of the flavonoids including catechin, quercetin, and kaempferol, was quantified using a linear gradient liquid chromatography (Figure 1). The amount of (+)-catechin in the specimen was significant at 53.86 mg/g (5.39% dry weight). Additionally, trace amounts of quercetin

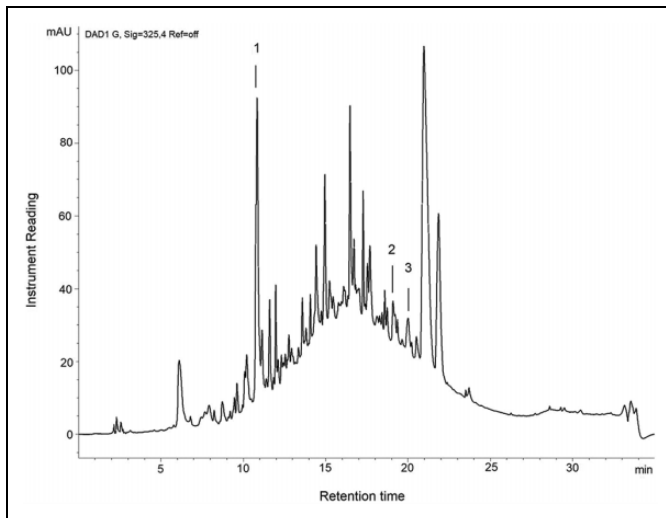


Figure 1. Chromatographic fingerprinting of CcME. The chromatogram shows the rich composition of phytochemicals in CcME. Several flavonoids were detected at ultra-violet 325 nm with (+)-catechin (1), quercetin (2), and kaempferol (3) eluting at 10.6, 18.79, and 20.20 min, respectively.

and kaempferol were detected at 1.38 mg/g (0.14% dry weight) and 2.26 mg/g (0.23% dry weight) (Figure 1).

CcME Inhibitory Effects on the TNBC MDA-MB-231 Cell Viability and Cytotoxicity

After 24 h of TNBC MDA-MB-231 cell exposure to various concentrations (25–200 $\mu\text{g}/\text{mL}$) of CcME, the percentage cell viability and cytotoxicity were determined, based on the measurement of the ATP molecules produced by metabolically active cells, and on the dead-cell protease activity, respectively. A gradual inhibition of the TNBC cell viability, in a dose-dependent manner, was observed as well as increasing concentrations of CcME, compared to a high viability level in the untreated cells, the control (Figure 2A). Exposing the cells to 50 $\mu\text{g}/\text{mL}$ CcME, resulted in a significant inhibition of 20% ($p < 0.05$) cell viability, and significant decreases of 36% ($p < 0.01$) and 64% ($p < 0.001$) in cell viability were observed after the addition of higher concentrations (100–200 $\mu\text{g}/\text{mL}$) of CcME, compared to the control, respectively (Figure 2A). In terms of the cytotoxicity, a minor effect of the CcME was observed resulting in a significant increase by 20% ($p < 0.001$) cytotoxicity after the addition of 200 $\mu\text{g}/\text{mL}$ of CcME, compared with the untreated and DMSO-treated TNBC cells (Figure 2B).

CcME Pro-Apoptotic Effects in the TNBC MDA-MB-231 Cells

To investigate the anti-proliferative-related molecular mechanisms exerted by CcME, we tested the potential pro-apoptotic properties of various concentrations of CcME in TNBC MDA-MB-231 cells. We analyzed the apoptosis status of the

untreated and CcME-treated TNBC cells, based on the detection of the FITC-labeled Annexin V bound to the phosphatidylserine, exposed on the outer plasma membrane leaflet, with the binding of the PE-labeled PI to the cellular DNA. The TNBC cells were exposed to 25–50 and 100 $\mu\text{g}/\text{mL}$ of CcME, which led to a significant inhibition of 10–15% in cell viability, with a slight increase in the percentage in early (5% increase) and late (13% increase) apoptotic cells, compared with the control and DMSO-treated cells (Figure 3). Tested at the highest concentration (200 $\mu\text{g}/\text{mL}$), the CcME decreased cell viability by 50%, and a 50% induction of apoptosis was measured, with 40% of the cell population in early apoptosis and 10% in late apoptosis, compared with the high viable status of the untreated and DMSO-treated TNBC cells (Figure 3).

CcME Pro-Apoptotic Effects Are Associated With Mitochondrial Permeability Transition Pore Opening and Caspase-3 Cleavage Activities

To investigate the deeper CcME pro-apoptotic effects in the TNBC MDA-MB-231 cells, we assessed the caspase-3 cleavage activity and used the mitochondrial transition pore opening assay to explore the intrinsic apoptotic pathway. Using confocal fluorescence microscopy, the increased mitochondrial outer membrane permeability activity, allowing the release of cytochrome *c*, was visualized in the TNBC cells treated with 100 and 200 $\mu\text{g}/\text{mL}$ CcME. Representative photomicrographs indicated that the 100 $\mu\text{g}/\text{mL}$ and 200 $\mu\text{g}/\text{mL}$ CcME increased the mitochondrial outer membrane permeability by 2.61-fold ($p < 0.05$) and 4.53-fold ($p < 0.01$), observed by the emission of green fluorescence from the mitochondrial calcein dye spread in the whole apoptotic cells, compared to the control cells (Figure 4A). To confirm whether the executioner caspase was cleaved during the apoptotic process, the CcME-exposed TNBC cells were lysed and the whole lysate proteins were extracted. The pro-caspase-3/cleaved caspase-3 was detected using Western blot analysis. The pro-caspase-3 protein expression was decreased, with the increasing concentrations of CcME, the cleavage of caspase-3 appeared after cell exposure to 50 $\mu\text{g}/\text{mL}$ of CcME. The highest expression level of the cleaved caspase-3 was observed in the TNBC cells exposed to 200 $\mu\text{g}/\text{mL}$ of CcME, compared to the controls (Figure 4B).

CcME Primarily Up-Regulates Cytochrome *c*, Catalase and Cycle-Dependent Kinase *p21* Expression in the Apoptotic Proteins in TNBC MDA-MB-231 Cells

We assessed the level of expression of several key apoptotic proteins in the CcME-exposed TNBC MDA-MB-231 cells, compared to the basal level detected in the untreated cells with an apoptosis-related protein array. In the non-treated TNBC cells (Figures 5A₁ & 5A₄), a moderate level of expression of the main pro-apoptotic components including Bad, cytochrome *c*, tumor necrosis factor (TNF)-related-apoptosis-inducing ligand (TRAIL)-2, heat shock protein (HSP)60, and phospho-p53

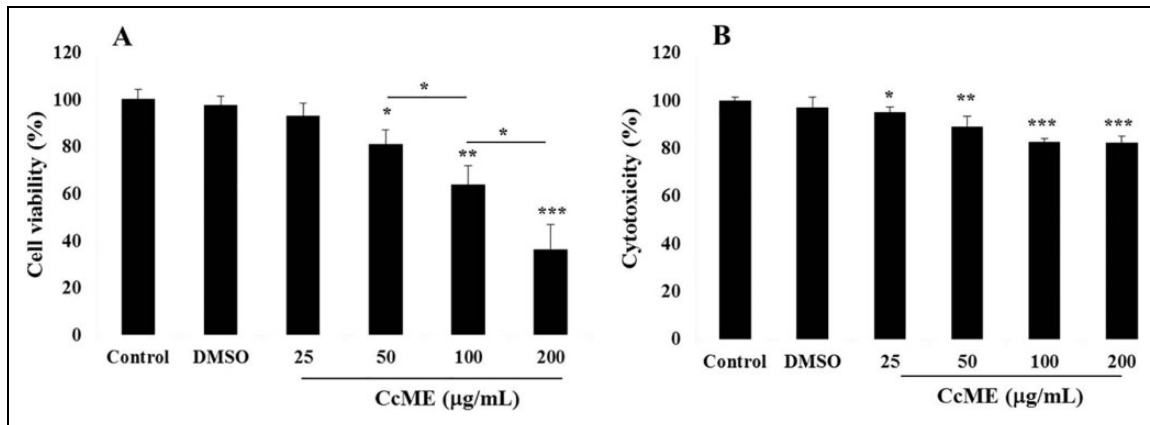


Figure 2. Effects of CcME on TNBC MDA-MB-231 cell viability (A) and CcME cytotoxicity (B). Cell viability and cytotoxicity were determined using CellTiter-glo[®] and CytoTox-Glo[®] kits, respectively. Untreated cells are considered as the control. The data are presented as mean \pm SD of 3 separate experiments. (*), (**), and (***) signify a statistically significant difference ($p < 0.05$, $p < 0.01$, and $p < 0.001$, respectively) from the control.

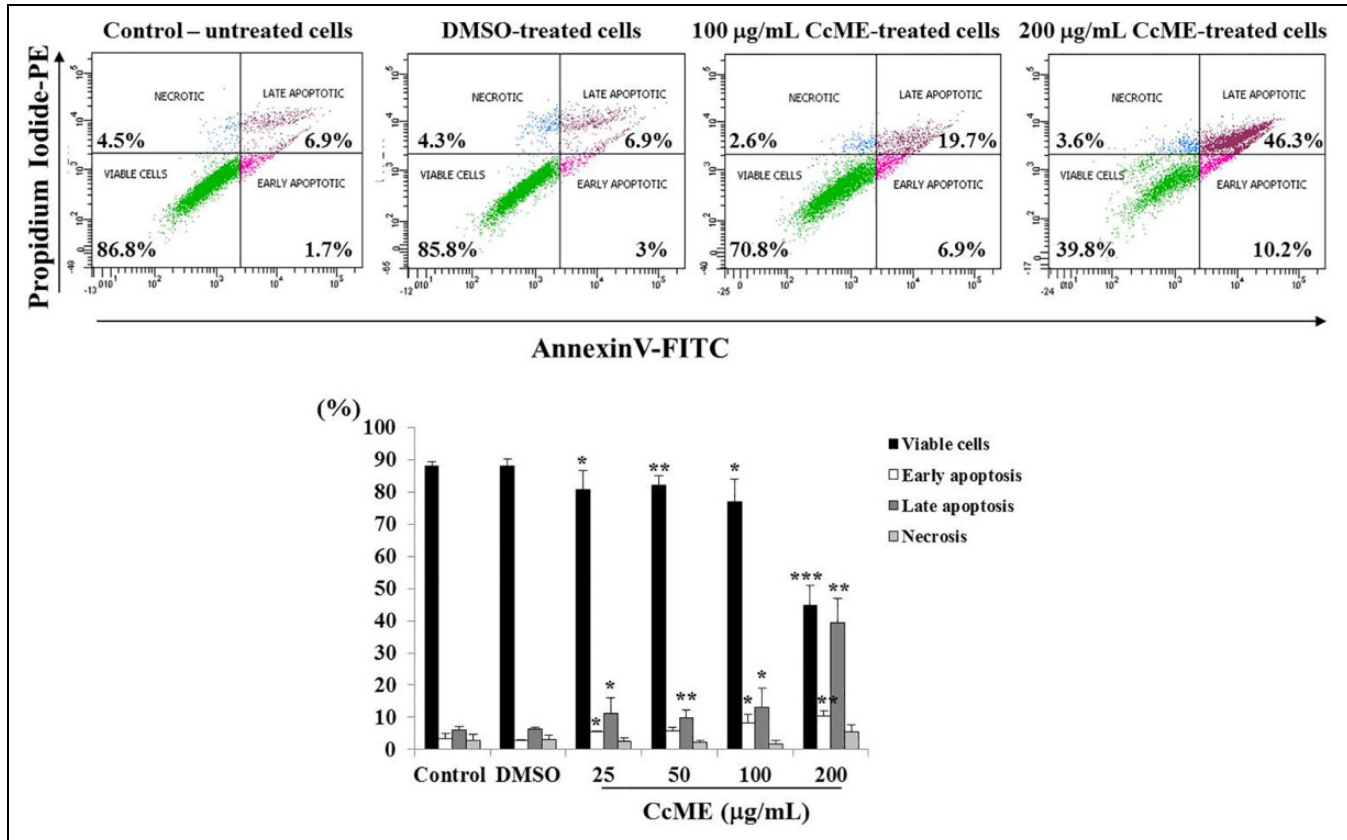


Figure 3. Effects of CcME on the induction of apoptosis in TNBC MDA-MB-231 cells. Representative scatter plots with percentage of viable cells, early apoptotic, late apoptotic, and necrotic cells. Bar graphs indicate the percentage apoptosis of TNBC cells in the presence or absence of CcME. The data are presented as mean \pm SD of 3 separate experiments. (*), (**), and (***) signify a statistically significant difference ($p < 0.05$, $p < 0.01$, and $p < 0.001$, respectively) from the control.

(S46) was detected, with the procaspase-3, catalase, phospho-p53 (S392), SMAC/Diablo, and the anti-apoptotic HSP27, highly expressed (Figures 5A₁&5A₄). A weak expression of the cyclin-dependent kinase protein, such as p21 and p27, was assessed in the healthy non-treated TNBC cells (Figures

5A₁&5A₄). An addition of 100 µg/mL (Figure 5A₂) and of 200 µg/mL (Figure 5A₃) CcME confirmed the increase in the cleaved-caspase-3, catalase, and of cytochrome c, with a decrease in the expression of Bad, HSP60, and survivin (Figure 5A₄). With all the apoptotic proteins, a concomitant increase of

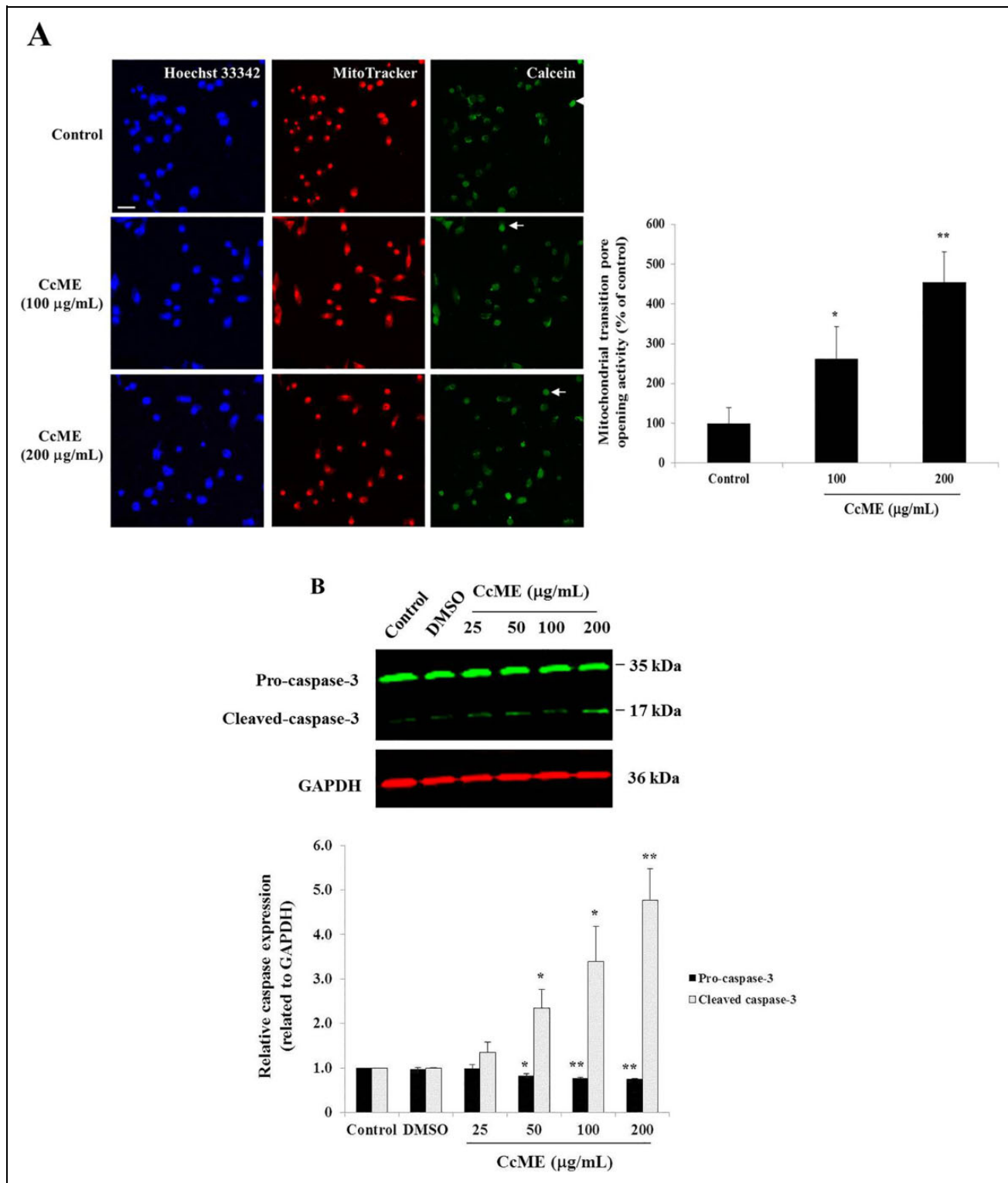


Figure 4. Involvement of apoptotic pathways in CcME-treated TNBC MDA-MB-231 cells. A, Representative photomicrographs showing the permeabilization of the mitochondrial outer membrane in TNBC cells (top) with or without 100-200 µg/mL of CcME. Enhancement of the mitochondrial outer membrane permeability is pointed by arrows showing examples of cells undergoing apoptosis with quenched green fluorescence of calcein. The bar graph indicates the mitochondrial transition pore activity expressed in percentage, as compared with the control. Scale bar = 50 µm. B, Representative Western blot showing CcME-induced caspase-3 cleavage in TNBC cells in a dose-dependent manner, as compared to the quasi-absence of cleaved caspase-3 detected in non-treated cells, the control. The bar graph presents the mean expression level of pro-caspase-3 and cleaved caspase-3. The data are presented as mean \pm SD of 3 separate experiments. (*), (**), and (***) signify a statistically significant difference ($p < 0.05$, $p < 0.01$, and $p < 0.001$, respectively) from the control.

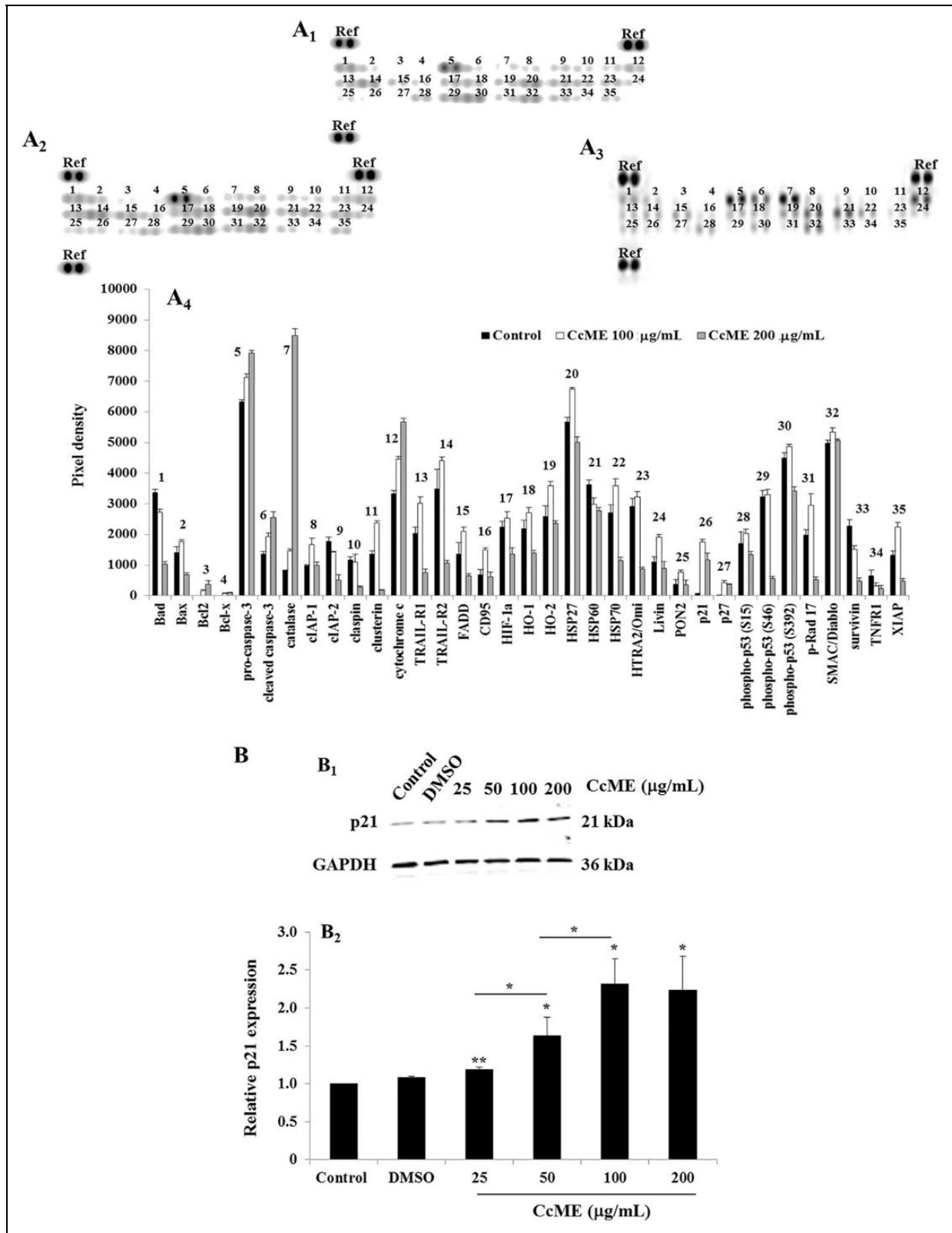


Figure 5. Effects of CcME on apoptosis-related protein expression in TNBC MDA-MB-231 cells. A, Representative apoptosis array membranes of 35 apoptosis-related proteins in untreated TNBC cells (A₁) or cells treated with either 100 µg/mL (A₂) or 200 µg/mL (A₃) CcME. The bar graph (A₄) shows the relative expression in TNBC cells of the relevant apoptotic proteins. B, Representative Western blot showing CcME-induced p21 up-regulation in TNBC cells in a dose-dependent manner, as compared with the basal level of p21 detected in the control. The bar graph presents the mean expression level of p21. The data are presented as mean ± SD of 3 separate experiments. (*), (**), and (***) signify a statistically significant difference ($p < 0.05$, $p < 0.01$, and $p < 0.001$, respectively) from the control.

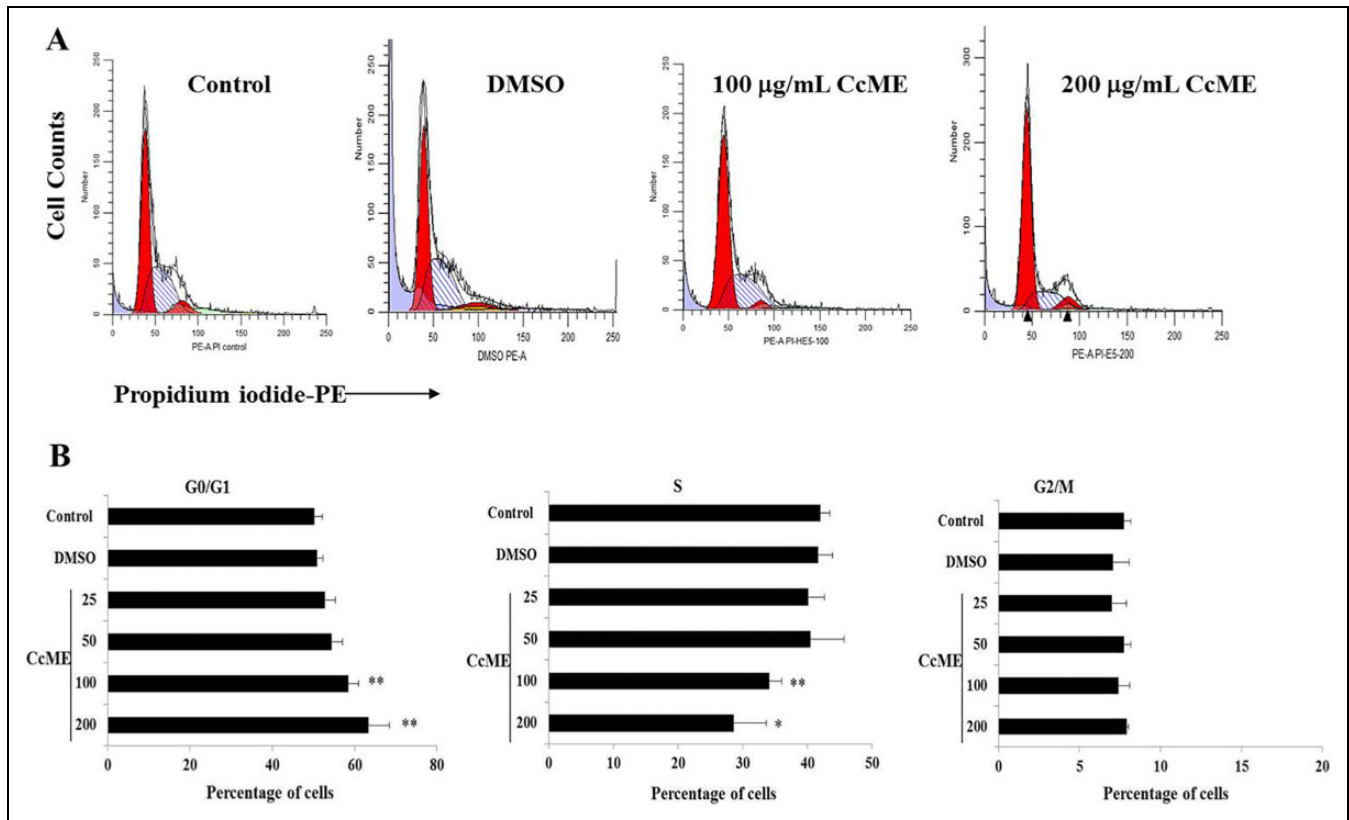


Figure 6. Effects of CcME on TNBC MDA-MB-231 cell-cycle-phase progression. Representative histograms (established by ModFit software) of cell distribution in cell cycle of untreated TNBC cells or cells treated with DMSO, 100 and 200 µg/mL CcME. The bar graphs present the percentage of cells at each cell cycle of TNBC cells in the presence or absence of CcME. The data are presented as mean \pm SD of 3 separate experiments. (*) and (***) signify a statistically significant difference ($p < 0.05$ and $p < 0.01$, respectively) from the control.

cyclin-dependent kinase p21 was observed in the TNBC cells exposed to 100 µg/mL CcME (Figures 5A₂&5A₄), with a slight decrease in the expression when the cells were treated with the highest CcME concentration (Figures 5A₃ &5A₄), compared to the basal expression level detected in the non-treated TNBC cells (Figures 5A₁&5A₄). To verify the CcME-induced p21 in the TNBC cells, using a Western blot, a dose-dependent enhancement of the p21 protein expression in TNBC cells, treated with increasing CcME concentrations (25-50-100 µg/mL) was observed (Figure 5B). Notably, with 200 µg/mL of CcME, there was no difference in the level of p21 expression, detected in the TNBC cells exposed to 100 µg/mL of CcME (Figure 5B).

CcME Induces TNBC MDA-MB-231 Cell Growth Arrest at G₀/G₁

Known as a cell death mechanism, cell cycle progression was analyzed using flow cytometry after staining the cellular DNA with PI, a vital dye. The quantity of DNA detected was proportional to the percentage of cells at a certain cell-cycle-phase progression. Compared with the proportion of TNBC MDA-MB-231 cells detected in the untreated condition or the DMSO-treated cells, CcME, tested at 100 and 200 µg/mL,

significantly increased the proportions of cells at the G₀/G₁ phase, with a decrease in the proportion of cells in the S phase (Figure 6). The G₂/M phase contained a similar proportion of TNBC cells in all the conditions used (Figure 6).

CcME Stimulates ROS Production in the TNBC MDA-MB-231 Cells

ROS, one of the main toxic radicals, causes anti-proliferative effects including apoptosis and cell cycle progression arrest.^{21,22,36} We evaluated ROS production, using the cellular red fluorescence-labeled ROS detection kit, after 90 min of the TNBC MDA-MB-231 cell exposure to various concentrations (25-200 µg/mL) CcME. Similar levels of generated ROS were detected in the untreated and DMSO-exposed TNBC cells, and a significant induction of ROS generation was triggered by the addition of H₂O₂, the positive control (Figure 7). The addition of increasing doses of CcME led to a gradual production of ROS, in a dose-dependent manner, by 4.0-fold at the highest dose (200 µg/mL) CcME, compared with the ROS level detected in the untreated and DMSO-treated TNBC cells (Figure 7). The impact of the ROS in the CcME-induced apoptosis was checked after pre-treating the cells with the ROS scavenger, N-acetylcystein (NAC), followed by cell exposure to 200

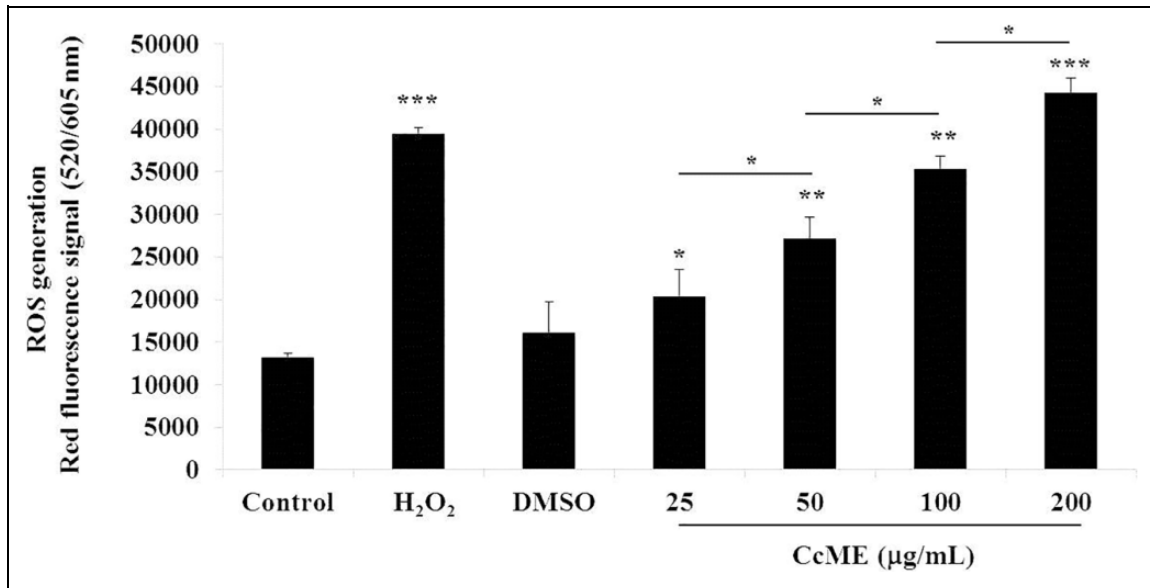


Figure 7. CcME stimulates cellular ROS generation in TNBC MDA-MB-231 cells. Unexposed cells and cells exposed to H₂O₂ (strong inducer), DMSO, various concentrations of CcME for 90 min were analyzed for generated ROS detection in TNBC cells. The bar graph presents the relative detection of generated ROS in all aforementioned experimental conditions. The data are presented as mean \pm SD of 3 separate experiments. (*), (**), and (***) signify a statistically significant difference ($p < 0.05$, $p < 0.01$, and $p < 0.001$, respectively) from the control.

$\mu\text{g/mL}$ CcME to the positive control for apoptosis induction, the staurosporine (STS)-treated cells (Figure 8). After 24 h incubation and FACS analysis, the NAC pre-treatment prevented the STS-induced apoptosis, but did not modify the CcME-induced apoptosis, compared to apoptosis induced by CcME alone (Figure 8).

Discussion

Natural products, especially herbal medicines, are a focus for the development of therapies against cancer development and progression.³⁷⁻⁴¹ A review by Newman and Cragg⁴² concluded that since the 1940s, 85 of 131 FDA-approved non-synthetic anticancer drug treatments have been derived from natural products or derivatives. We measured the biological impact of endotoxin-free CcME on the most aggressive TNBC cell line, MDA-MB-231. We investigated the impact of various concentrations of CcME on the TNBC cell line viability and cytotoxicity, as well as its anti-proliferative effects. We investigated the potential underlying cancer cell death mechanisms by analyzing apoptosis and the apoptosis-related protein expression in the CcME-treated TNBC MDA-MB-231 cells, compared to healthy viable untreated cells. Exerting a low cytotoxic effect, the CcME exerted pro-apoptotic effects in the TNBC cells and upregulated the cyclin-dependent kinase inhibitor p21, a key protein causing cell growth arrest at the G₀/G₁ phase. The over-production of ROS, detected in the CcME-treated TNBC cells, was not implicated in the CcME-induced apoptosis.

The *C. comosum* sample used throughout this study was obtained from a local vendor, obtained from the central region

of Saudi Arabia. The 3 flavonoids of (+)-catechin, quercetin, and kaempferol were chosen to be detected in the CcME to determine the quality of the herbal medicine, compared to reported flavonoid levels in *C. comosum*. Previous studies identified (+)-catechin, quercetin, and kaempferol in the aerial part of *C. comosum*.^{26,27} The amount of (+)-catechin in the specimen was determined chromatographically and was 53.86 mg/g, lower than reported in literature. For instance, the extract of the leaves was reported to contain 113 mg/g (11.3%) (+)-catechin in hydrolyzed methanolic *C. comosum* extract.²⁶ An explanation of this difference could be attributed to several factors, including natural variation, as well as the method or solvent of extraction used. However, the content of the quercetin assessed from the methanolic extract of *C. comosum* leaves in the present study, confirmed a similar prior chemical analysis. Kiani et al.⁴³ found 2.1 mg/g (0.21%) quercetin in the aerial part of *C. comosum*. No report for the kaempferol concentration in the aerial parts of *C. comosum* is available.

The TNBC cell line was exposed to different concentrations of CcME and we measured the effects on the cell viability, apoptosis including apoptosis-related proteins, caspase- and mitochondrial-based pathways, cell cycle and cellular ROS generation. Tested at increasing concentrations between 25 and 200 $\mu\text{g/mL}$, the CcME significantly decreased the TNBC cell viability in a dose-dependent manner. These findings confirm the anti-proliferative effect of *C. comosum* on cancer cell lines using the hormone-dependent breast cancer cell line (MCF-7) and the hepatocarcinoma cell line (HepG2) as reported by Ahmed et al.²⁹ Several flavonoids from the hydroalcoholic extract of the aerial part of *C. comosum* caused the anti-proliferative effect, specifically quercetin.²⁹ Flavonoids are

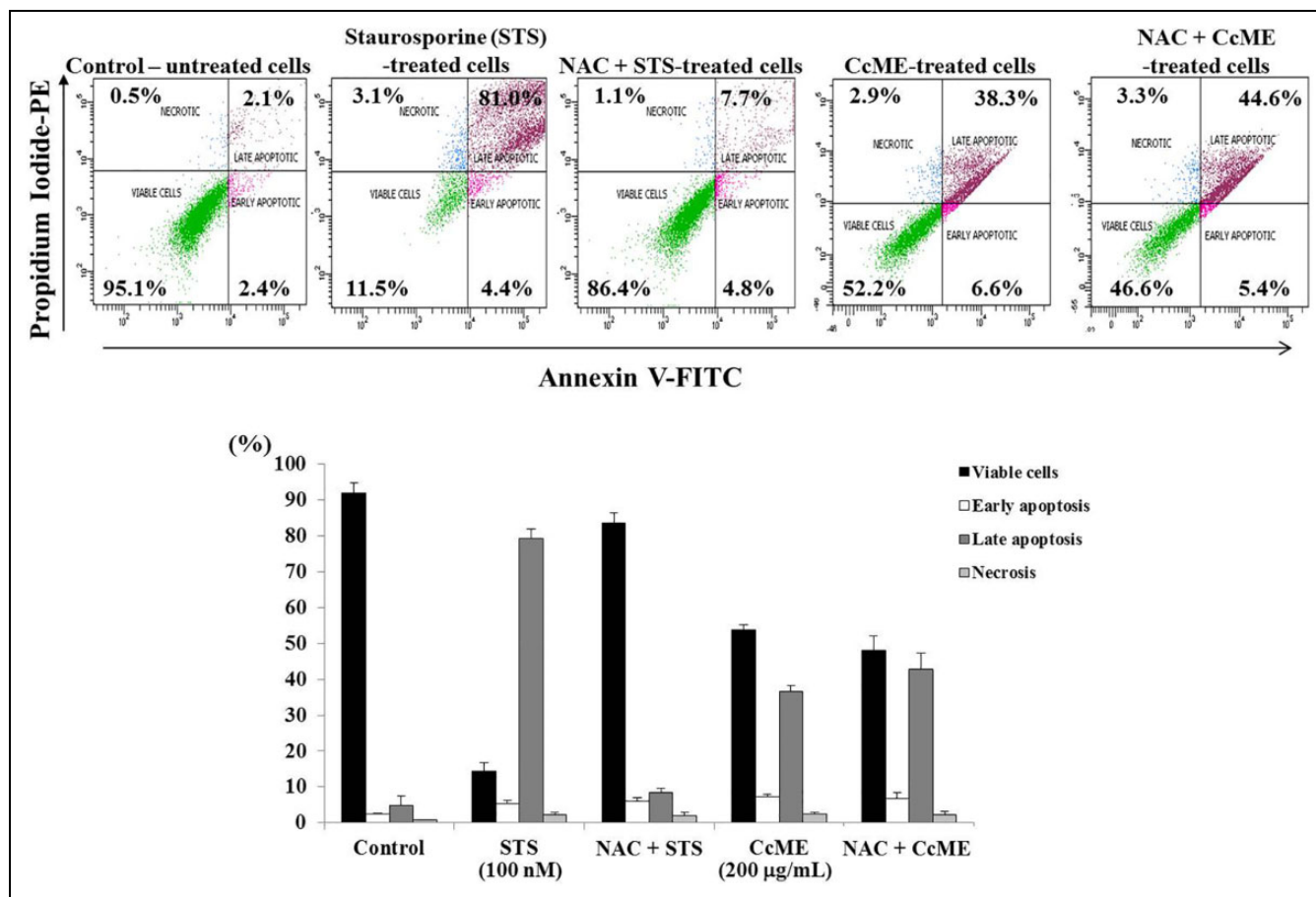


Figure 8. ROS is not essential for CcME-induced apoptosis in TNBC MDA-MB-231 cells. Representative scatter plots showing the impact of ROS scavenger on CcME-induced apoptosis in MDA-MB-231 cells. Bar graphs present the percentage apoptosis of MDA-MB-231 cells in the aforementioned conditions.

polyphenolic metabolites known for their cytotoxic effect against cancer cell proliferation through the induction of apoptosis and cell growth arrest. This effect was demonstrated with hepatocarcinoma cells exposed to maleic anhydride derivatives and quercetin.⁴⁴ Screening the effect of all or the main bioactive phytochemical compounds of CcME on TNBC MDA-MB-231 cell growth would increase the anti-carcinogenic efficiency through cell growth arrest and apoptosis induction.

Using the FACS analysis and the apoptosis protein array, the apoptotic status of the CcME-treated TNBC cells was measured after 24 h incubation. A small proportion, 10%-15% of the TNBC cell population underwent apoptosis at low concentrations (25-50 $\mu\text{g}/\text{mL}$), however at 100 $\mu\text{g}/\text{mL}$ of CcME, a significant induction of apoptosis, including early apoptosis (10% of the TNBC cell population) and late apoptosis (40% of the TNBC cell population) was observed by the addition of 200 $\mu\text{g}/\text{mL}$ CcME. Of note, any cell in late apoptosis irreversibly results in cell death.¹⁶ Based on the apoptosis protein array, most of the proteins listed were slightly upregulated, including the main pro-apoptotic proteins such as cleaved-caspase 3. With no expression of the cell cycle dependent kinase inhibitor in the healthy TNBC cells, the exposure of the cells to 100-200 $\mu\text{g}/\text{mL}$ of CcME induced the expression of

p21 and p27, both cell cycle-dependent kinase inhibitors known to cause cell growth arrest in the G_0/G_1 phase.¹⁷ The upregulation of p21 in the CcME-treated TNBC cells was confirmed with a Western blot, which displayed a gradual increase of the p21 expression level in a dose-dependent manner, compared to the p21 basal expression level detected in the untreated TNBC cells and cells treated with DMSO. Recent literature confirms that many plant-based bioactive compounds induce apoptosis and cell cycle arrest.⁴⁵⁻⁴⁷ The up-regulation of p21, caused by the TNBC exposure to 100-200 $\mu\text{g}/\text{mL}$ CcME, increased the percentage of cells in the G_0/G_1 phase, with a significant decrease of cells in the S phase. As expected, there was no change in the percentage of cells in the G_2/M phase, in all experimental conditions. An investigation of the deeper molecular mechanisms underlying the CcME-induced apoptosis and cell cycle arrest was done after the blockade of the caspase activity and the p21 protein expression.

Known to cause cell damage resulting in cell death, including apoptosis,^{21,48} cellular ROS production was evaluated after exposing the TNBC cells for 90 min to different doses of CcME. At the lowest CcME concentration (25 $\mu\text{g}/\text{mL}$), a significant increase of cellular ROS generation was detected, compared to the cellular ROS generated in the control cells. Numerous

studies reported the pro-oxidative properties of natural compounds, but only a few studies assessed the ROS production at a cellular level.^{49,50} Cellular ROS are tightly generated reactive byproducts of aerobic respiration, cell metabolism and are implicated in the redox homeostasis and diverse pathways of cellular signaling.^{18,19} Generated from external (cytokines, growth factors activating NADPH oxidase) or internal (mitochondrial respiratory chain) sources, an excessive level of ROS molecules contribute to carcinogenesis by damaging the lipids, proteins, and nucleic acids. A moderate ROS level plays a key role in apoptosis, cell survival, and cell differentiation.^{51,52} In the present study, the pre-treatment of the TNBC cells with the ROS scavenger NAC, demonstrated that the ROS was not implicated in the CcME-induced apoptosis. These findings are in agreement with previous studies analyzing pro-apoptotic anti-cancer natural-based drugs.³⁶ Deeper investigation of the ROS impact in CcME-induced cell cycle arrest would be of interest.

Conclusion

We have demonstrated that CcME exerts anti-proliferative effects against TNBC MDA-MB-231 cells through the induction of apoptosis, involving the activation of the mitochondrial-dependent apoptotic pathway and through cell cycle arrest at the G₀/G₁ phase, associated with p21 up-regulation. The current findings indicate that CcME contains potent anti-cancerous phytochemical compounds, which could later be identified through the establishment of structure-function relationships, based on a comparative study with other alternative traditional plant extract-based medication.⁵³ However, *in vivo* studies are required to confirm the CcME anti-proliferative activity, and to investigate any potential anti-metastatic activities against the highly invasive TNBC.

Abbreviations

CcME	<i>Calligonum comosum</i> methanolic extract
Cdk	cycle-dependent kinase
DMSO	dimethyl sulfoxide
FACS	fluorescence-activated cell sorter
FBS	fetal bovine serum
FITC	fluorescein isothiocyanate
HER2	human epidermal growth factor receptor 2
HPLC	high-performance liquid chromatography
NAC	N-acetylcystein
PE	phycoerythrin
PI	propidium iodide
ROS	reactive oxygen species
SDS-PAGE	sodium dodecyl sulfate-polyacrylamide gel electrophoresis
TNBC	triple-negative breast cancer

Authors' Note

ZA and SMN conceived the study. WBY, HA, MA, MoA, AA, MT, AN, MHA performed the assays, collected the data and analyzed the data. SMN, ZA, and SA wrote the paper.

Acknowledgments

We would like to thank Dr Saleh Alehaideb from the Experimental Medicine Department and Mr. Thadeo Trivilegio from the Department of Medical Research Core Facility and Platforms at King Abdullah International Medical Research (KAIMRC) for their expertise in the use of the confocal laser scanning microscopy and flow cytometry, respectively. This study was financially supported by KAIMRC; grant # RC16/175/R.


Declaration of Conflicting Interests


The author(s) declared no potential conflicts of interest with respect to the research, authorship, and/or publication of this article.

Funding

The author(s) disclosed receipt of the following financial support for the research, authorship, and/or publication of this article: This study was fully financially supported by KAIMRC, grant number # RC16/175/R.

ORCID iDs

Abeer Albaz  <https://orcid.org/0000-0002-1098-8652>

Sabine Matou-Nasri  <https://orcid.org/0000-0003-4372-2903>

References

- Ghoncheh M, Pournamdar Z, Salehiniya H. Incidence and mortality and epidemiology of breast cancer in the world. *Asian Pac J Cancer Prev*. 2016;17(S3):43-46.
- Bray F, Ferlay J, Soerjomataram I, Siegel RL, Torre LA, Jemal A. Global cancer statistics 2018: GLOBOCAN estimates of incidence and mortality worldwide for 36 cancers in 185 countries. *CA Cancer J Clin*. 2018;68(6):394-424.
- Diana A, Franzese E, Centonge S, Carlino F, Della Corte CM. Triple-negative breast cancers: systematic review of the literature on molecular and clinical features with a focus on treatment and innovative drugs. *Curr Oncol*. 2018;29(10):895-902.
- Lee A, Djamgoz MBA. Triple negative breast cancer: emerging therapeutic modalities and novel combination therapies. *Cancer Treat Rev*. 2018;62:110-122.
- Masoud V, Pages G. Targeted therapies in breast cancer: new challenges to fight against resistance. *World J Clin Oncol*. 2017;8(2):120-134.
- Bonavita E, Pelly VS, Zelenay S. Resolving the dark side of therapy-driven cancer cell death. *J Exp Med*. 2018;215(1):9-11.
- Varghese E, Samuel SM, Abotaleb M, Cheema S, Mamtani R, Busselberg D. The "Yin and Yang" of natural products in anticancer therapy of triple-negative breast cancer. *Cancers (Basel)*. 2018;10(10):346.
- Mitra S, Dash R. Natural products for the management and prevention of breast cancer. *Evid Based Complement Alternat Med*. 2018;2018:ID8324696.
- Greenwel M, Rahman PK. Medicinal plants: their use in anticancer treatment. *Int J Pharm Sci Res*. 2015;6(10):4103-4112.
- Iqbal J, Abbasim BA, Mahmood T, et al. Plant-derived anticancer agents: a green anticancer approach. *Asian Pac J Biomed*. 2017;7(12):1129-1150.
- Cheng YY, Hsieh CH, Tsai TH. Concurrent administration of anticancer chemotherapy drug and herbal medicine on the

- perspective of pharmacokinetics. *J Food Drug Anal.* 2018;26(2S):588-595.
12. Wang F, Wang H, Sun X, Li M. Apoptosis-induction is a novel therapeutic strategy for gastrointestinal and liver cancers. *Curr Gene Ther.* 2015;15(2):193.
 13. Pistrutto G, Trisciuglio D, Ceci C, Garufi A, D'Orazi G. Apoptosis as anticancer mechanism: function and dysfunction of its modulators and targeted therapeutic strategies. *Aging (Albany NY).* 2016;8(4):603-619.
 14. Baig S, Seevasant I, Mohamad J, Mukheem A, Huri HZ, Kamarul T. Potential of apoptotic pathway-targeted cancer therapeutic research: where do we stand? *Cell Death Dis.* 2016;7(1):e2058.
 15. Merino VF, Cho S, Nguyen N, et al. Induction of cell cycle arrest and inflammatory genes by combined treatment with epigenetic, differentiating, and chemotherapeutic agents in triple-negative breast cancer. *Breast Cancer Res.* 2018;20(1):145.
 16. Elmore S. Apoptosis: a review of programmed cell death. *Toxicol Pathol.* 2007;35(4):495-516.
 17. Lim S, Kaldis P. Cdks, cyclins and CKIs: roles beyond cell cycle regulation. *Development.* 2013;140(15):3079-3093.
 18. Roy J, Galano JM, Durand T, Le Guennec JY, Lee JC. Physiological role of reactive oxygen species as promoters of natural defenses. *FASEB J.* 2017;31(9):3729-3745.
 19. Sies H. Hydrogen peroxide as a central redox signaling molecule in physiological oxidative stress: oxidative eustress. *Redox Biol.* 2017;11:613-619.
 20. Boonstra J, Post JA. Molecular events associated with reactive oxygen species and cell cycle progression in mammalian cells. *Gene.* 2004;337:1-13.
 21. Ivanova D, Zhelev Z, Aoki I, Bakalova R, Higashi T. Overproduction of reactive oxygen species—obligatory or not for induction of apoptosis by anticancer drugs. *Chin J Cancer Res.* 2016;28(4):383-396.
 22. Mateen S, Moin S, Khan AQ, Zafar A, Fatima N. Increased reactive oxygen species formation and oxidative stress in rheumatoid arthritis. *PLoS One.* 2016;11(4):e0152925.
 23. Nissanka N, Moraes CT. Mitochondrial DNA damage and reactive oxygen species in neurodegenerative disease. *FEBS Lett.* 2018;592(5):728-742.
 24. Taia WK, El-Etaby MO. Taxonomical study in the desert plant *Calligonum comosum* L'Her from two different locations in Saudi Arabia. *Asian J Plant Sci.* 2006;5(4):570-579.
 25. Liu XM, Zakaria MN, Islam MW, et al. Anti-inflammatory and anti-ulcer activity of *Calligonum comosum* in rats. *Fitoterapia.* 2001;72(5):487-491.
 26. Abdo W, Hirata A, Shukry M, et al. *Calligonum comosum* extract inhibits diethylnitrosamine-induced hepatocarcinogenesis in rats. *Oncol Lett.* 2015;10(2):716-722.
 27. Badria FA, Ameen M, Akl MR. Evaluation of cytotoxic compounds from *Calligonum comosum* L. growing in Egypt. *Z Naturforsch C.* 2007;62(9-10):656-660.
 28. Shalabi M, Khilo K, Zakaria MM, Elsebaei MG, Abdo W, Awadin W. Anticancer activity of *Aloe vera* and *Calligonum comosum* extracts separately on hepatocellular carcinoma cells. *Asian Pacif J Tropic Biomed.* 2015;5:375-381. doi:10.1016/S2221-1691(15)30372-5
 29. Ahmed H, Moawad A, Owis A, AbouZid S, Ahmed O. Flavonoids of *Calligonum polygonoides* and their cytotoxicity. *Pharm Biol.* 2016;54(10):2119-2126.
 30. Sharaf H, Matou-Nasri S, Wang Q, et al. Advanced glycation endproducts increase proliferation, migration and invasion of the breast cancer cell line MDA-MB-231. *Biochim Biophys Acta.* 2015;1852(3):429-441.
 31. Hammoudeh SM, Hammoudeh AM, Hamoudi R. High-throughput quantification of the effect of DMSO on the viability of lung and breast cancer cells using an easy-to-use spectrophotometric trypan blue-based assay. *Histochem Cell Biol.* 2019;152(1):75-84.
 32. Rameshbabu S, Messaoudi SA, Alehaideb ZI, et al. *Anastatica hierochuntica* (L.) methanolic and aqueous extracts exert antiproliferative effects through the induction of apoptosis in MCF-7 breast cancer cells. *Saudi Pharm J.* 2020;28(8):985-993.
 33. El-Obeid A, Alajmi H, Harbi M, et al. Distinct anti-proliferative effects of herbal melanin on human acute monocytic leukemia THP-1 cells and embryonic kidney HEK293 cells. *BMC Complement Med Ther.* 2020;20(1):154.
 34. Matou-Nasri S, Rhaban Z, Albuyaijan H, et al. CD95-mediated apoptosis in Burkitt's lymphoma B-cells is associated with Pim-1 down-regulation. *Biochim Biophys Acta Mol Basis Dis.* 2017;1863(1):239-252.
 35. Matou-Nasri S, Sharaf H, Wang Q, et al. Biological impact of advanced glycation endproducts on estrogen receptor-positive MCF-7 breast cancer cells. *Biochim Biophys Acta.* 2017;1863(11):2808-2820.
 36. Masgras I, Carrera S, de Verdier PJ, et al. Reactive oxygen species and mitochondrial sensitivity to oxidative stress determine induction of cancer cell death by p21. *J Biol Chem.* 2012;287(13):9845-9854.
 37. Balunas MJ, Kinghorn AD. Drug discovery from medicinal plants. *Life Sci.* 2005;78(5):431-441.
 38. Sagar SM, Yance D, Wong RK. Natural health products that inhibit angiogenesis: a potential source for investigational new agents to treat cancer-Part 1. *Curr Oncol.* 2006;13(1):14-26.
 39. Cragg GM, Grothaus PG, Newman DJ. Impact of natural products on developing new anti-cancer agents. *Chem Rev.* 2009;109(7):3012-3043.
 40. Chen CY. TCM Database@Taiwan: the world's largest traditional Chinese medicine database for drug screening in silico. *PLoS One.* 2011;6(1):e15939.
 41. Manju K, Jat RK, Anju G. A review on medicinal plants used as a source of anticancer agents. *Int J Drug Res Technol.* 2017;2:6. ISSN 2277-1506. <http://www.ijdr.com/index.php/drug-research-and-technology/article/view/a-review-on-medicinal-plants-used-as-a-source-of-anticancer-agents>
 42. Newman DJ, Cragg GM. Natural products as sources of new drugs from 1981 to 2014. *J Nat Prod.* 2016;79(3):629-661.
 43. Kiani K, Lamardi SN, Ostad SN, et al. Quantification of quercetin, catechin, and β -sitosterol, antioxidant and acute toxic effects of *Calligonum comosum* L'Her, different parts extract. *Int J Adv Res.* 2016;4(8):380-388.
 44. Carrasco-Torres G, Baltiérrez-Hoyos R, Andrade-Jorge E, Villa-Treviño S, Trujillo-Ferrara JG, Vásquez-Garzón VR. Cytotoxicity, oxidative stress, cell cycle arrest, and mitochondrial

- apoptosis after combined treatment of hepatocarcinoma cells with maleic anhydride derivatives and quercetin. *Oxid Med Cell Longev*. 2017;2017:2734976.
45. Kim SA, Kang OH, Kwon DY. Cryptotanshinone induces cell cycle arrest and apoptosis of NSCLC cells through the PI3K/Akt/GSK-3 β pathway. *Int J Mol Sci*. 2018;19(9):2739.
46. Liu Q, Cao Y, Zhou P, et al. Panduratin A inhibits cell proliferation by inducing G0/G1 phase cell cycle arrest and induces apoptosis in breast cancer cells. *Biomol Ther (Seoul)*. 2018;26(3):328-334.
47. Smolensky S, Rhodes D, McVey DS, et al. High-polyphenol sorghum bran extract inhibits cancer cell growth through ROS induction, cell cycle arrest, and apoptosis. *J Med Food*. 2018;21(10):990-998.
48. Zheng WL, Wang BJ, Wang L, et al. ROS-mediated cell cycle arrest and apoptosis induced by Zearalenone in mouse Sertoli cells via ER stress and the ATP/AMPK pathway. *Toxins (Basel)*. 2018;10(1):E24.
49. Wang J, Luo B, Li X, et al. Inhibition of cancer growth *in vitro* and *in vivo* by a novel ROS-modulating agent with ability to eliminate stem-like cancer cells. *Cell Death Dis*. 2017;8(6):e2887.
50. Xu X, Dang Z, Sun T, Zhang S, Zhang H. The role of reactive oxygen species in screening anticancer agents. *Cancer Transl Med*. 2018;4(1):35-38. <http://www.cancertm.com/text.asp?2018/4/1/35/226172>
51. Redza-Dutordoir M, Averill-Bates DA. Activation of apoptosis signaling pathways by reactive oxygen species. *Biochim Biophys Acta*. 2016;1863(12):2977-2992.
52. Yilmazer A. Cancer cell lines involving cancer stem cell populations respond to oxidative stress. *Biotechnol Rep (Amst)*. 2018;17:24-30.
53. Khan T, Ali M, Khan A, et al. Anticancer plants: a review of the active phytochemicals, application in animal models, and regulatory aspects. *Biomolecules*. 2020;10(1):47.